Experimental And Theoretical Study Performance Of Combined Dual Pass Photovoltaic Thermal Air Heater

Dr. Ebrahim M. Alfegi ***Dr. Alhadi A. Abosbaia***
Dept. Of Mechanical Engineering
Faculty of Engineering- Zawia
Zawia University

ABSTRACT :

Photovoltaic thermal (PV/T) solar air heater is a collector that combines solar thermal collector and photovoltaic cells in one single hybrid generating unit. It generates both thermal and electrical energies simultaneously. Two configurations of the hybrid photovoltaic thermal solar air heaters were designed, fabricated and their performances were studied experimentally and theoretically.

In considered designs the air flowing either on both sides of the absorber plate with Compound Parabolic Concentrator (CPC) located parallel to the air flow and rectangular fins attached to the

back side of the absorber in a single pass (Configuration 1) and without CPC (with fins only) (Configuration 2). In these configurations, air enters through both sides of the absorber in single pass and in double duct at the same time. Five coupled of unsteady nonlinear partial differential equations were formulated to predict the performance of PV/T solar air heater at different parameters and conditions.

Comparison between the experimental and theoretical results has been carried out and close agreement has been observed. The combined efficiency varies from 42.56 % to 69.59 % for configuration 1, and from 38.67 % to 63.34 % for configuration 2. The results indicated that the collector with CPC and fins have higher efficiency than collector with fins only.

Keywords: *solar collector, pv/t, single pass, double pass, cpc, fin, efficiency*

Nomenclature :

A_c	collector area	(m^2)
A_f	channel flow area	(m^2)
C_p	specific heat of air	(J/kg K)
CR	concentration ratio of CPC	
D_h	hydraulic diameter	(m)
f	friction factor	
h_f	height of the fin	(m)
h_c	convective heat transfer coefficient	(W/m2 K)
h_r	radiative heat transfer	(W/m2 K)
H_1	height of the upper channel	(m)

H_2	height of the lower channel	(m)
I	radiation intensity	(W/m^2)
k	thermal conductivity	(W/m^2 k)
L	length of the collector	(m)
$\dot{m}$	air mass flow rate	(kg/s)
n`	average number of reflection for radiation passing through CPC inside the acceptance-half angle	
t	time	(sec)
t_f	thickness of the fin	(m)
t_g	glass thickness	(m)
t_p	absorber plate thickness	(m)
t_{bp}	back plate thickness	(m)
T	temperature	(^oC)
U_b	back plate overall heat loss transfer coefficient	(W/m^2 K)
W	width of the collector	(m)

Subscripts :

a	ambient
ab(T)	top absorber surface
ab(B)	bottom absorber surface
bp	back plate
c	convective
f	fin
f1	working Fluid at first channel
f2	working Fluid at second channel
g	glass cover
i	inlet
o	outlet
P	reflector

PV	photovoltaic cell
p	absorber plate
r	radiative
s	sky
tot	total
w	wind
x	x-direction

Greek letters :

α	absorptance	
ΔP	pressure drop (N/m^2)	
ε	emmissivity	
τ	transmittance	
ρ	density (kg/m^3)	
σ	Stefan-Boztman constant	($W/m^2 k^4$)
η_{th}	thermal efficiency	(%)
η_{pv}	photovoltaic efficiency	(%)
$\eta_{PV/T}$	combined photovoltaic thermal efficiency	(%)
μ	viscosity	($N s/m^2$)

Introduction :

Several configurations of solar air heaters have been developed in literature. A number of theoretical as well as experimental studies have been made on the hybrid photovoltaic thermal collector systems with air as heat transfer fluid. In PV/T air collector the circulating air stream passes either in single pass configuration, or in double pass

configuration, carrying away excess heat. Thus, the electrical energy output increases, and overall efficiency of the system increases too.

Many studies have been made in single pass photovoltaic thermal collector. Florschuetz [1] extended the Hottel–Willer analytical model for flat plate collectors to analyse the combined photovoltaic thermal collector with simple modification of the conventional parameters of the original model by assuming that a liner correlation between efficiency of solar cell array and its temperature over its operating temperature range. Cox and Raghuraman [2] performed computer simulations to optimize the design of flat plate PV/T solar air collector at Lincoln Laboratory to increase the efficiency of electrical and thermal system.

The use of a concentrator on the photovoltaic thermal collector is attracting research attention to produce collector design that has better performance. Garg et al. [3] produced the first theoretical study on photovoltaic thermal collector using plane booster reflectors. This hybrid system consists of a flat plate solar air heater mounted with photovoltaic cells and two plan booster reflectors above and below the collector. Prakash [4] developed a mathematical model for predicting the performance of photovoltaic thermal system. He presented a Transient analysis based on energy balance equations of the model for various fluid flow rates and fluid duct depths. Takashima et al. [5] proposed new model of photovoltaic thermal system to get electricity and thermal energy by evaluated the quality of electricity and thermal energy using the concept of exergy.

The performance of single and double glass configurations PV/T air heating collectors based on the steady state analytical solution of a differential equation that yields the working fluid temperature along the direction of fluid flow was investigated by Garg

and Adhikar [6]. Garg and Adhikar [7] investigated a transient computer simulation model for the analysis of a solar PV/T hybrid collector with air as working fluid. Tiwari et al. [8] evaluated an experimental study of thermal model of PV/T system to study the performance of unglazed PV/T model for composite climate of India. Tonui and Tripanagnostopoulos [9] carried out experimental tests on two commercial PV modules configured as PVT/Air solar collectors and run under forced and natural air flow modes to keep the electrical efficiency at acceptable level and to achieve higher thermal efficiency. Tonui and Tripanagnostopoulos [10] also investigated the performance of two low cost heat extraction improvement modifications in the channel of PV/T air system to keep the electrical efficiency at acceptable level and to achieve higher thermal efficiency. Tiwari and Sodha [11] carried out an experimental study for different configurations of hybrid air collectors which are considered as glazed and unglazed PV/T air heaters with and without tedlar.

Research of the PV/T collector proceeded for the double pass air collector configuration also carried out. Sopian et al. [12] has built a new design of photovoltaic thermal collector with flat plate and two air passages. Garg and Adhikar [13] investigated a theoretical analysis for the modeling thermal and electrical processes of PV/T air heating collector coupled with CPC under steady state based on energy balance equations for the various components of the system. Sopian et al. [14] studied theoretical and experimental on a double pass photovoltaic thermal solar collector suitable for solar drying applications under steady state closed form solution to determine the outlet and mean photovoltaic panel temperature for the differential equations. Tripanagnostopoulos et al. [15] built and tested various photovoltaic thermal collector models with and without glass cover.

The performance of these collectors was improved using booster diffuse reflector made from aluminium sheets. Othman et al [16] investigated the performance of double pass PV/T air heater with fins fixed in the bottom of absorber plate to increase the heat transfer to the air and enhance the efficiency of the system. The system was studied theoretically and experimentally under steady state conditions. In this paper, an experimental and theoretical study of two dual pass photovoltaic thermal air heaters has been developed. The concept of the these configurations of PV/T collectors are shown in figures 1 and 2.

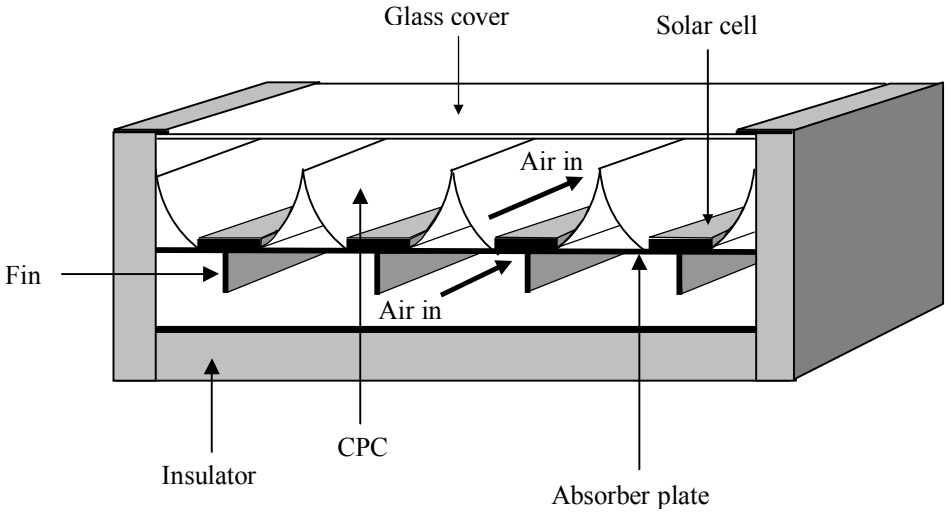

Figure 1: Schematic diagram of a single pass, double duct photovoltaic thermal solar air collector with CPC and fins

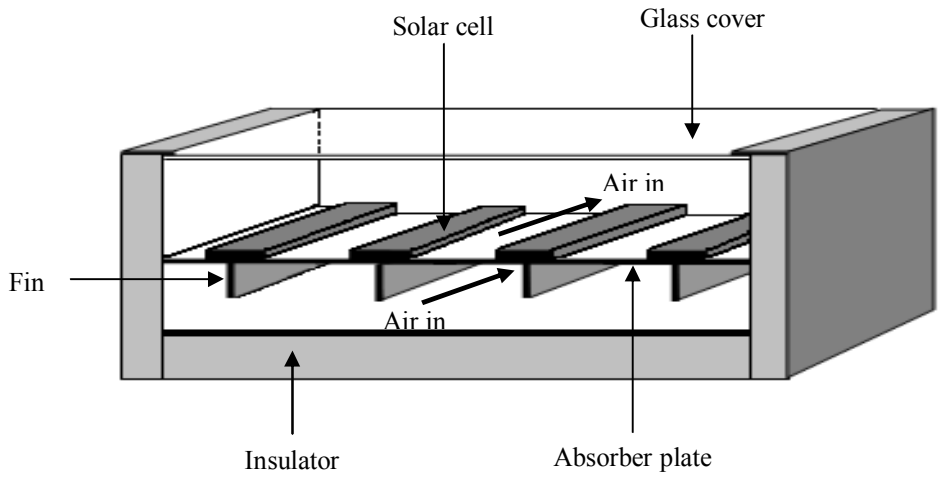

Figure 2: Schematic diagram of a single pass, double duct photovoltaic thermal solar air collector with fins only

Experimental setup :

The schematic diagram of the experimental setup for single pass, double duct PV/T air heater is shown in figure 3. The collectors have three essential static components: a glass plate on the top, 36 monocrystalline cells arranged in 4 rows and connected in series were pasted to an absorber plate made from aluminum and coated with black paint, and bottom plate insulated with glass wool. The collector has dimensions of 0.855 m width and 1.22 m length. The high of the upper channel is 0.165 m and 0.125 m for the lower channel.

The total area covered by solar cells is 0.38 m^2. 29 rectangular fins also made from aluminum, each has 0.025 m high, 1.22 m length, and 0.001 m thickness with fin density of 38.4 fins/m attached along the length of the back of the PV/T panel. CPC with concentration ratio (CR) of 1.86 is used as a reflector and located parallel to the air flow in Configuration 1. Collectors were tested under solar simulator has 23 tungsten halogen lamps each rated of 500 W. The collectors have

been operated at varying inlet temperature, mass flow rate, and intensity of radiation conditions. The inlet temperature varies from 30 to 35^{o}C, the mass flow rate varies from 0.0316 to 0.09 kg/s, and intensity of radiation varies from 400 to 700 W/m^{2}.

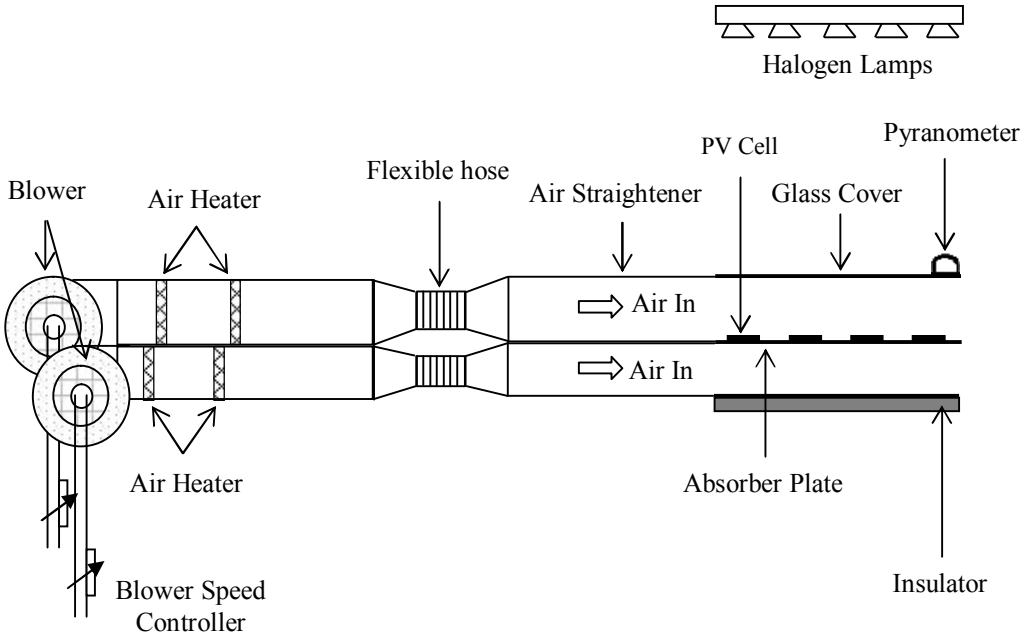

Figure 3: Schematic diagram of experimental setup for single pass, double duct (PV/T) air heater

Mathematical model :

In this paper, a mathematical modeling and solution procedure for predicting the electrical, thermal, and combined performance of the PV/T collectors is presented. This model can predict the performance of the collector easily if several parameter design and changed environment parameter for the purpose of changing scale and optimization of the collector. This parameter includes the long parameter (L), the deepness of first channel (H_1) which is shaped by

the glass cover and the absorber plate attached with photovoltaic cell and CPC component above it, deepness of second channel (H_2) shaped by absorber plate at the finned part with the back plate of the collector, air mass flow rate through the collector and also the intensity of radiation received on the surface of the collector. Analysis of five coupled of transient nonlinear partial differential equations have been done in this study. The schematic diagram of the two configurations collectors with heat transfer coefficients is shown in figures 4 through 5.

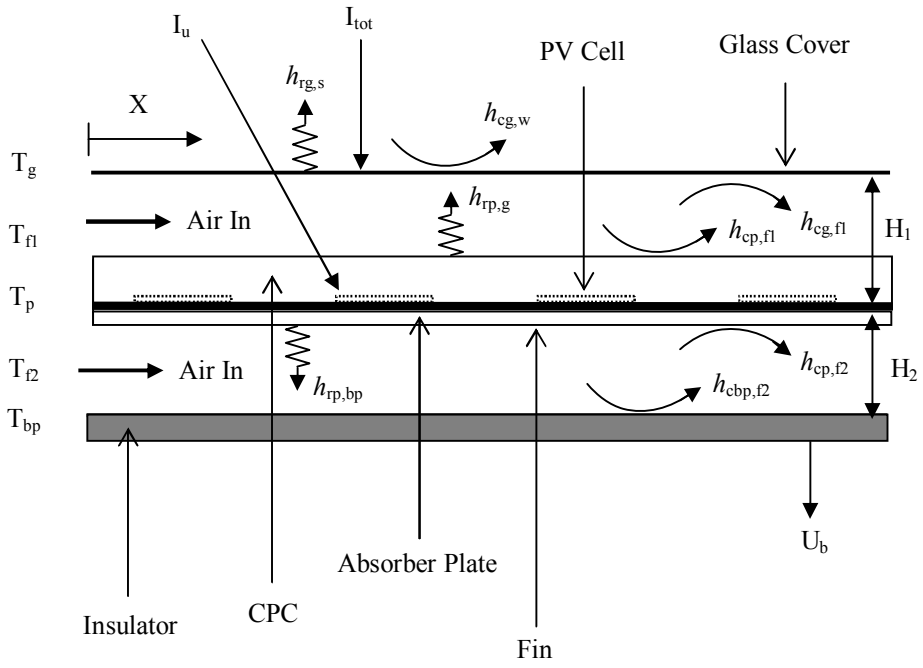

Figure 4: Schematic diagram of heat transfer coefficients in the collector with CPC and fins

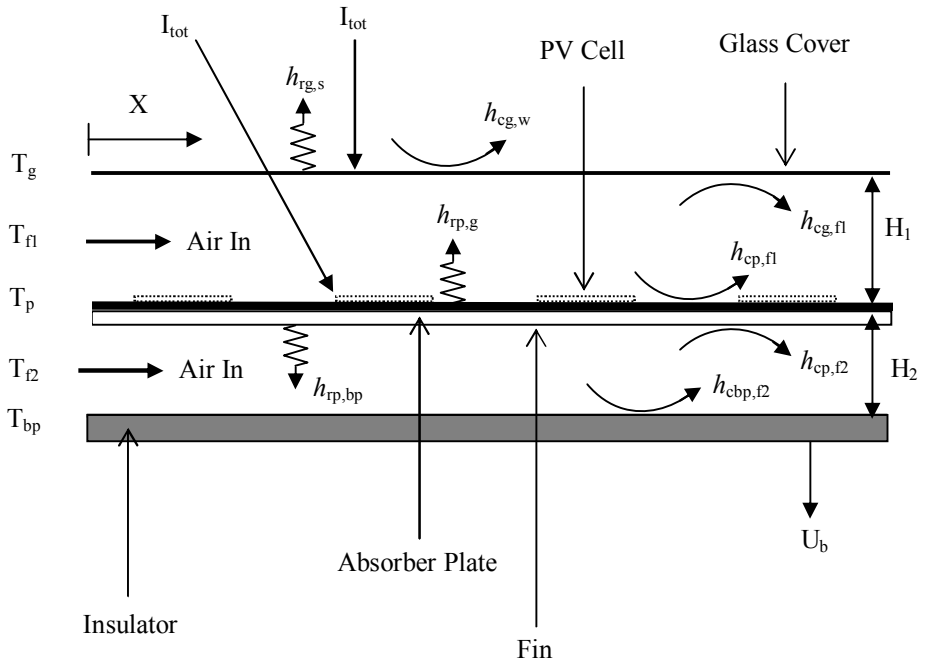

Figure 5: Schematic diagram of heat transfer coefficients in the collector with fins only

Energy balance equations :

a) Energy Balance for the Collectors With CPC and Fins

The transient energy balance equations for this configuration can be written as follows,

1. For the glass cover:

$$t_g \rho_g C_{pg} \frac{\partial T_g}{\partial t} = \alpha_g \mathrm{I_{tot}}(\mathrm{CR})(1+\tau_g \mathrm{P_p P_R^{2n'}}) + \mathrm{h}_{rg,s}(T_s - T_g) + h_{cg,w}(T_w - T_g) + h_{cg,f1}(T_{f1} - T_g) + h_{rg,p}\frac{A_{ab\,(T)}}{A_c}(T_p - T_g) \quad (1)$$

2. For the air stream in upper channel:

$$H_1\rho_{f1}C_{p_{f1}}\frac{\partial T_{f1}}{\partial t}=\frac{-\dot{m}_{f1}C_{p_{f1}}}{W}\frac{\partial T_{f1}}{\partial x}+h_{cg,f1}(T_g-T_{f1})+h_{cp,f1}\frac{A_{ab(T)}}{A_c}(T_p-T_{f1}) \quad (2)$$

3. For the absorber plate:

$$\begin{aligned} t_p\rho_p C_{p_p}\frac{\partial Tp}{\partial t}&=\tau_g\alpha_p \mathrm{I_u}\,(1-P)(CR)\mathrm{P}_R^{n'}d(1+(\frac{\mathrm{P}_p\mathrm{P}_g\mathrm{P}_R^{2n'}}{CR}))+\\ &\tau_g\alpha_{pv}\,\mathrm{I_u}(1-\eta_{pv})P(CR)\mathrm{P}_R^{n'}d(1+(\frac{\mathrm{P}_{pv}\mathrm{P}_g\mathrm{P}_R^{2n'}}{CR}))+\\ &h_{cp,f1}\frac{A_{ab(T)}}{A_c}(T_{f1}-T_p)+h_{rp,g}\frac{A_{ab(T)}}{A_c}(T_g-T_p)+\\ &h_{cp,f2}\frac{A_{ab(B)}}{A_c}\eta_p(T_{f2}-T_p)+h_{rp,bp}\frac{A_{ab(B)}}{A_c}(T_{bp}-T_p) \end{aligned} \quad (3)$$

Where:

$$I_u=\frac{I_{tot}}{CR}$$

4. For the air stream in lower channel:

$$H_2\rho_{f2}C_{p_{f2}}\frac{\partial T_{f2}}{\partial t}=\frac{-\dot{m}_{f2}C_{p_{f2}}}{W}\frac{\partial T_{f2}}{\partial x}+h_{cbp,f2}(T_{bp}-T_{f2})+h_{cp,f2}\frac{A_{ab(B)}}{A_c}\eta_p(T_p-T_{f2}) \quad (4)$$

5. For the back plate:

$$t_{bp}\rho_{bp}C_{p_{bp}}\frac{\partial T_{bp}}{\partial t}=U_b(\mathrm{T_a}-\mathrm{T_{bp}})+h_{cbp,f2}(T_{f2}-T_{bp})+h_{rp,bp}\frac{A_{ab(B)}}{A_c}(T_p-T_{bp}) \quad (5)$$

b) Energy Balance for the Collectors without CPC(with fins only)

The transient energy balance equations for this configuration can be written as follows,

1. For the glass cover:

$$t_g\rho_g C_{pg}\frac{\partial T_g}{\partial t}=\alpha_g \mathrm{I}+\mathrm{h}_{rg,s}(T_s-T_g)+h_{cg,w}(T_w-T_g)+h_{cg,f1}(T_{f1}-T_g)+h_{rg,p}(T_p-T_g) \quad (6)$$

2. For the air stream in upper channel:

$$H_1\rho_{f1}C_{p_{f1}}\frac{\partial T_{f1}}{\partial t}=\frac{-\dot{m}_{f1}C_{p_{f1}}}{W}\frac{\partial T_{f1}}{\partial x}+h_{cg,f1}(T_g-T_{f1})+h_{cp,f1}(T_p-T_{f1}) \quad (7)$$

3. For the absorber plate:

$$\begin{aligned} t_p\rho_p C_{p_p}\frac{\partial Tp}{\partial t}=&\tau_g\alpha_p \mathrm{I}(1-P)+\tau_g\alpha_{pv}I(1-\eta_{pv})P+h_{cp,f1}(T_{f1}-T_p)+h_{rp,g}(T_g-T_p)\\ &+h_{cp,f2}\frac{A_{ab(B)}}{A_c}\eta_p(T_{f2}-T_p)+h_{rp,bp}\frac{A_{ab(B)}}{A_c}(T_{bp}-T_p)\end{aligned} \quad (8)$$

Where:

$$\eta_{\mathrm{p}}=1-\frac{\mathrm{A}_{\mathrm{fin}}}{\mathrm{A}_{\mathrm{ab(B)}}}(1-\eta_f)$$

$$\eta_{\mathrm{f}}=\frac{\tanh \mathrm{mh}_{\mathrm{f}}}{\mathrm{mh}_{\mathrm{f}}}$$

$$\eta_{\mathrm{pv}}=\eta_{ref}(1-0.0054(T_{pav}-T_{ref}))$$

$$\mathrm{m}=\left(\frac{2\mathrm{h}_{\mathrm{c}}}{\mathrm{k}_{\mathrm{f}}t_f}\right)^{\frac{1}{2}}$$

4. For the air stream in lower channel:

$$H_2\rho_{f2}C_{p_{f2}}\frac{\partial T_{f2}}{\partial t}=\frac{-\dot{m}_{f2}C_{p_{f2}}}{W}\frac{\partial T_{f2}}{\partial x}+h_{cbp,f2}(T_{bp}-T_{f2})+h_{cp,f2}\frac{A_{ab(B)}}{A_c}\eta_p(T_p-T_{f2}) \quad (9)$$

5. For the back plate:

$$t_{bp}\rho_{bp}C_{p_{bp}}\frac{\partial T_{bp}}{\partial t}=U_b(\mathrm{T_a}-\mathrm{T_{bp}})+h_{cbp,f2}(T_{f2}-T_{bp})+h_{rp,bp}\frac{A_{ab(B)}}{A_c}(T_p-T_{bp}) \quad (10)$$

Collector thermal performance :

In this paper; there are two types of collectors that are collector without CPC (with fins only) and collector with CPC and fins.
The thermal performance of the collector without CPC is easy as follow,

$$\eta_{thermal}=\frac{m\cdot C_p\int(T_o-T_i)dt}{A_c\int Idt} \quad (11)$$

While the thermal performance of the collector with CPC and fins is as follow,

$$\eta_{thermal}=\frac{m\cdot C_p\int(T_o-T_i)dt}{A_c(CR)\int Idt} \quad (12)$$

Collector photovoltaic performance :

The electrical performance of the photovoltaic thermal collector without CPC can be written as,

$$\eta_{electrical}=\frac{\int P_E dt}{\int Idt} \quad (13)$$

While for photovoltaic thermal collector with CPC is given by Othman et al. (2005) as,

$$\eta_{electrical}=\frac{\int P_E dt}{(CR)\int I_{tot}dt} \quad (14)$$

Where:

$$P_E = (CR)PI_u\tau_c p_R^{n'} d\alpha_c \left(1 + \frac{p_{pv} p_c p_R^{2n'}}{CR}\right) \tag{15}$$

$$I_u = \frac{I_{tot}}{CR} = \frac{I_B + I_D}{CR} \tag{16}$$

Combiend performance for the pv/t solar collector :

The performance of the photovoltaic thermal collector is defined as the sum of the total thermal energy and electrical energy divided by the total radiation absorbed at surface collector. The performance of the photovoltaic thermal collector without CPC is,

$$\eta_{PV/T} = \eta_{thermal} + \eta_{electrical} \tag{17}$$

$$\eta_{PV/T} = \frac{\int m C_p (T_o - T_i) dt}{A_c \int Idt} + \frac{\int P_E dt}{\int Idt} \tag{18}$$

While photovoltaic thermal performance for collector with CPC and fins is given as,

$$\eta_{PV/T} = \frac{\int m C_p (T_o - T_i) dt}{A_c (CR) \int Idt} + \frac{\int P_E dt}{(CR) \int Idt} \tag{19}$$

Solution procedures :

Based on the first order forward scheme in time and second order central difference scheme in space to predict the PV/T solar air heater at different parameters and conditions, an explicit transient model was developed for the four configurations PV/T collectors. An explicit transient analysis can be worked on through solving the transient energy balance equations for the various collector components.

The energy balance equations are subjected to the following boundary conditions:

For x = 0, x = L,

$$\left.\begin{aligned} &\frac{\partial T_1}{\partial x}=\frac{\partial T_3}{\partial x}=\frac{\partial T_5}{\partial x}=0 \\ &T_{f1}(0,t)=T_{measured}(t) \qquad \left.\frac{\partial T_{f1}}{\partial x}\right|_{x=L,t=0}=0 \\ &T_{f2}(0,t)=T_{measured}(t) \qquad \left.\frac{\partial T_{f2}}{\partial x}\right|_{x=L,t=0}=0 \end{aligned}\right\} \tag{20}$$

The space interval [0,L] is decretized by the N_{x+1} following points xj = jδx where j = 0,1,…,N_x and δx=L/ N_x. Similarly, time interval [0,t] is divided by the instants tn = nδt where n = 0,1,…., N_t and δt = t/ N_t. We solve Equations (1) through (10) along with their boundary condition equation (20), the first order forward scheme and second order central difference scheme which, applied for example Equation (2) yields:

$$H_l\rho_{f1}C_{pf1}\left(\frac{T_{f1}^{j,n+1}-T_{f1}^{j,n}}{\Delta t}\right)=\frac{-\dot{m}_{f1}C_{pf1}}{W}\left(\frac{T_{f1}^{j+1,n}-T_{f1}^{j-1,n}}{2\Delta x}\right)+h_{cg,f1}(T_g-T_{f1})+h_{cp,f1}(T_p-T_{f1}) \tag{21}$$

The final formula for Equation (21) is as follow,

$$T_{f1}^{j,n+1}=T_{f1}^{j,n}+\left(\frac{\Delta t}{H_l\rho_{f1}C_{pf1}}\right)\left(\frac{-\dot{m}_{f1}C_{pf1}}{W}\left(\frac{T_{f1}^{j+1,n}-T_{f1}^{j-1,n}}{2\Delta x}\right)+h_{cg,f1}(T_g-T_{f1})+h_{cp,f1}(T_p-T_{f1})\right) \tag{22}$$

And proceed in the same way for Equations (1) and (3) through (10).

The simulation program is written using FORTRAN language computer programming. It can simulate the transient performance of the system at a time interval of 0.0001 minute. Its inputs require radiation intensity, mass flow rate, and inlet temperature while its outputs contain the temperature of the glass cover, absorber plate with photovoltaic cells, back plate, and air flow in both channels. The output data used to determine the efficiency of PV/T system. The flow chart in figure 6 shows the key steps in the simulation program is capable to determine the performance of photovoltaic thermal collectors with any input parameters changes.

The procedure of the solution which is used to analyse the performance of the PV/T collector is as follow: The temperatures T_g, T_{f1}, T_p, T_{f2}, T_{bp} at any point during time n=0 and n=1 are taken at inlet air temperature, and Physical properties of air (μ, ρ, k, C_p) and various radiative heat transfer coefficients according to the initial condition were calculated. To simplify the model, various convective heat transfer coefficients were assumed constant. The mathematic model has been built in this paper will be used in the theory of analysis to predict the performance of the PV/T collector which is built.

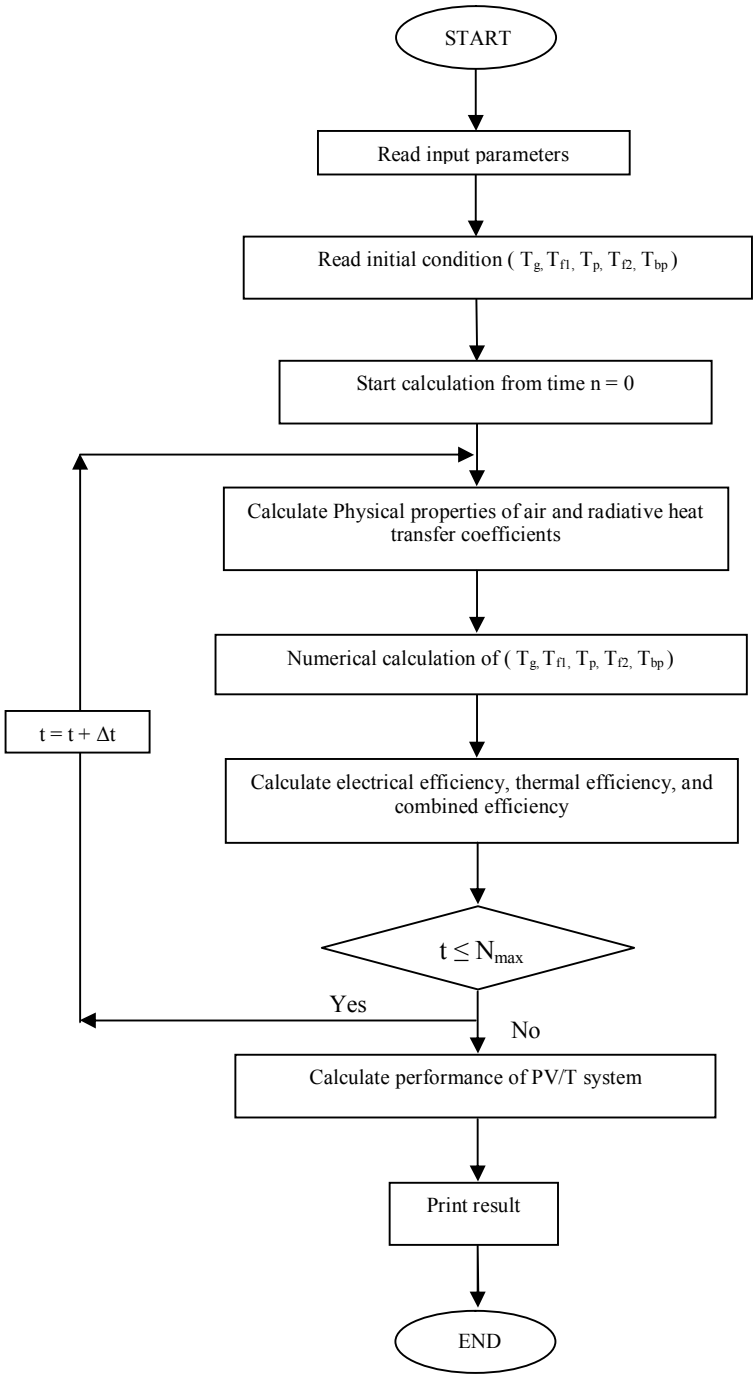

Figure 6: The flow chart to calculate the performance of the PV/T collector

Results and observations :

Performance characteristics curves for photovoltaic thermal collector for two configurations experimentally and theoretically have been plotted. Many parameters effect on the performance of the collector. Among the important parameters that influence the performance of the collector are: Temperature of the photovoltaic cell (T_s), air mass flow rate ($\dot{m}$), radiation intensity (I), depth of the first and second channel (H_1 and H_2), inlet temperature (T_i), packing factor of the photovoltaic cell (P), and collector length (Sopian 1997) [17]. In this analysis, collector length and packing factor have been kept constant along the experimental and theoretical analysis. Also, the upper and lower channels are kept constant at 0.165 and 0.125 m respectively. The comparisons between the various performance parameters for the considered PV/T Collectors are presented.

The Effect of Mass Flow Rate on the PV/T Solar Collector Efficiencies :

Changes in mass flow rate on photovoltaic cell temperature gives clear effect to the electrical efficiency. Also, Changes mass flow rate on temperature rise gives clear effect to the thermal efficiency of the PV/T collector. Effect on electrical and thermal efficiencies will give effect on combined efficiency which is the sum of electrical and thermal efficiencies. Figures 7 and 8 show the effect of mass flow on photovoltaic, thermal, and combined photovoltaic thermal efficiencies for different configurations designs at radiation intensity of 500 W/m^2 and inlet temperature of 30 ^oC. The experimental and theoretical results also have been shown.

Generally, it can be observed that collector operating at higher mass flow rate will increase the efficiencies. It can be observed also,

when collectors are operating at the same flow rate and inlet temperature of 30 ^{o}C the photovoltaic efficiency decreases as radiation intensity increase. However, under the same conditions the thermal efficiency increases with higher levels of radiation intensity. The combined photovoltaic efficiency also increases as radiation intensity increase.

As seen in figure 7, the experimental photovoltaic efficiency for collector with CPC is varied from 12.981% to 13.196%. The corresponding theoretical photovoltaic efficiency is varied from 13.466% to 13.611%. The experimental and theoretical thermal efficiencies are varied from 29.074% to 37.671% and from 42.644% to 42.876% respectively. Hence, the experimental and theoretical combined efficiencies are varied from 42.055% to 50.867% and from 56.11% to 56.487% respectively.

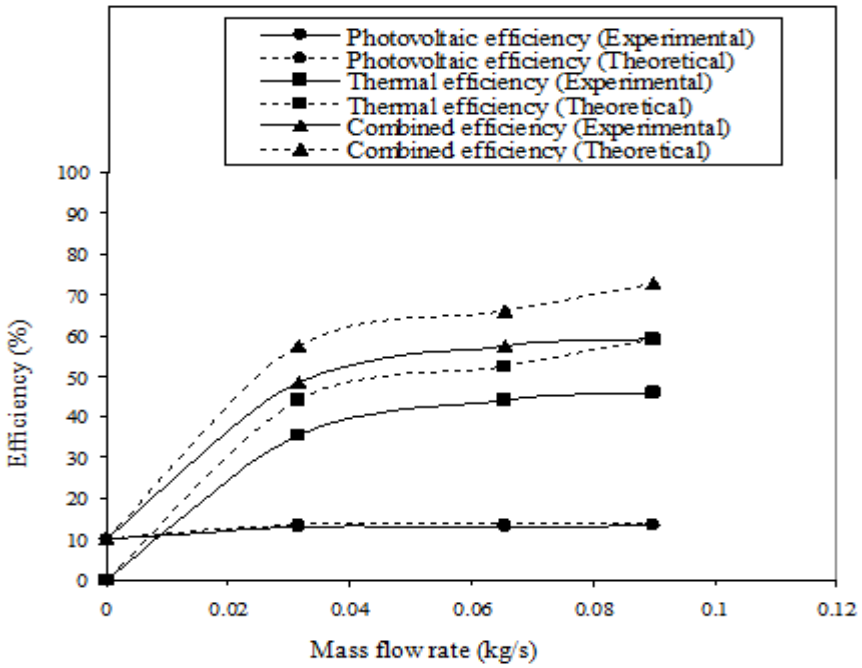

Figure 7: The effect of mass flow rate on photovoltaic, thermal, and combined photovoltaic thermal efficiencies for collector with CPC and fins

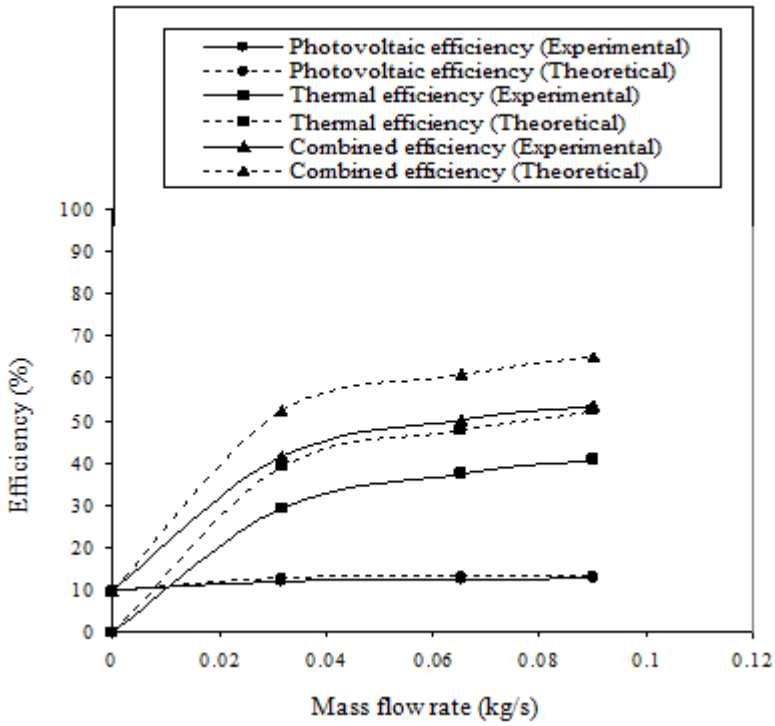

Figure 8: The effect of mass flow rate on photovoltaic, thermal, and combined photovoltaic thermal efficiencies for collector without CPC (with fins only)

The Effect of Temperature Rise on the Efficiencies :

The effect of the temperature rise ($T_o - T_i$) on the thermal efficiency (η_{th}) and on the combined efficiency (η_{PVT}) for different air mass flow rate for different configurations can be seen in Figures 9 through 12. The figures show the region in which the experiments have been conducted with four lines that indicate the limits for the mass flow rate and solar energy intensity. One of the lines shows the limit for mass flow rate that is less than 0.0316 kg/s. the other line indicates the limit for mass flow rate greater than 0.09 kg/s. Also shown in the figure are the limit lines for the solar intensity.

Therefore, the other two lines indicate values for solar intensity less than 400 W/m^2 and for solar intensity greater than 700 W/m^2. These figures are so useful and can be used to find the value of the temperature rise, thermal efficiency, and combined efficiency of the photovoltaic thermal collector if the air mass flow rate and solar intensity is known. The following example will illustrate the use of the figures, if air mass flow rate is fixed at 0.0655 kg/s and operating at solar intensity of 500 W/m^2.

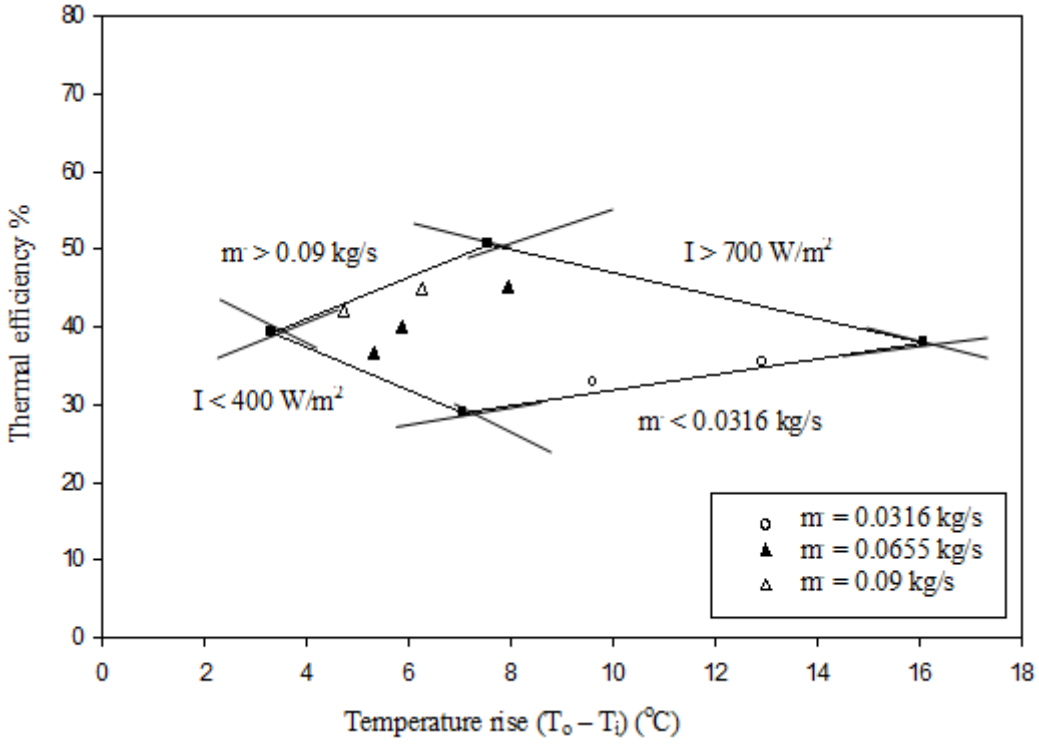

Figure 9: Effect of the temperature rise on the thermal efficiency for single pass, double duct PV/T with CPC and fins at various mass flow rates and [Ti = 30°C]

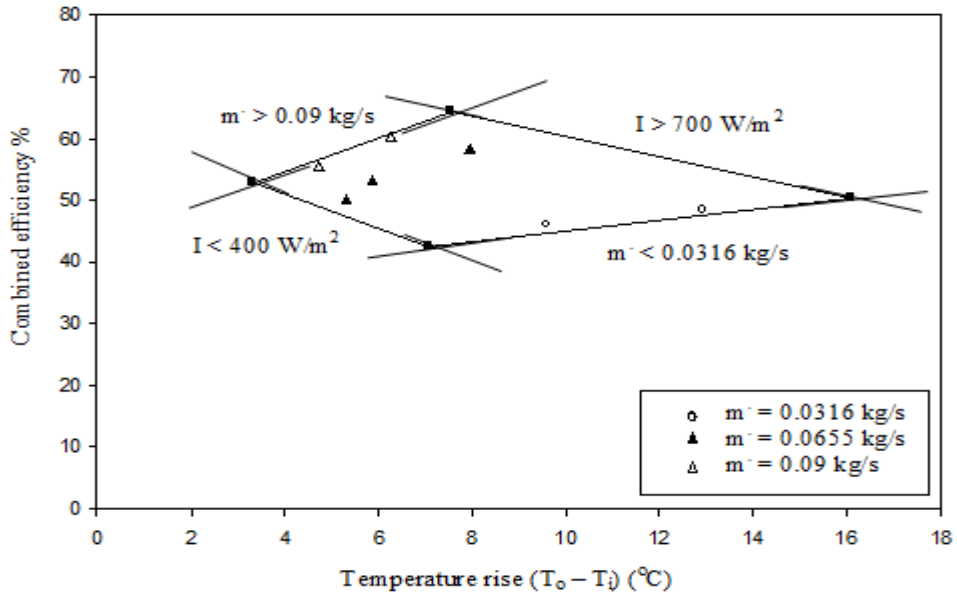

Figure 10: Effect of the temperature rise on the combined efficiency for single pass, double duct PV/T with CPC and fins at various mass flow rates and [Ti = 30°C]

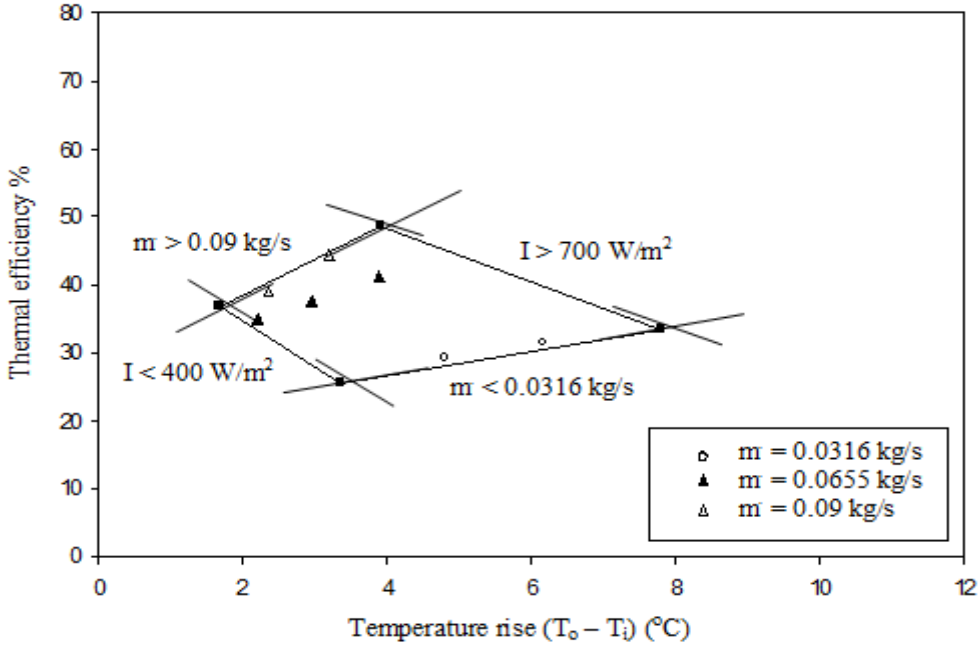

Figure 11: Effect of the temperature rise on the thermal efficiency for single pass, double duct PV/T without CPC at various mass flow rates and [Ti = 30°C]

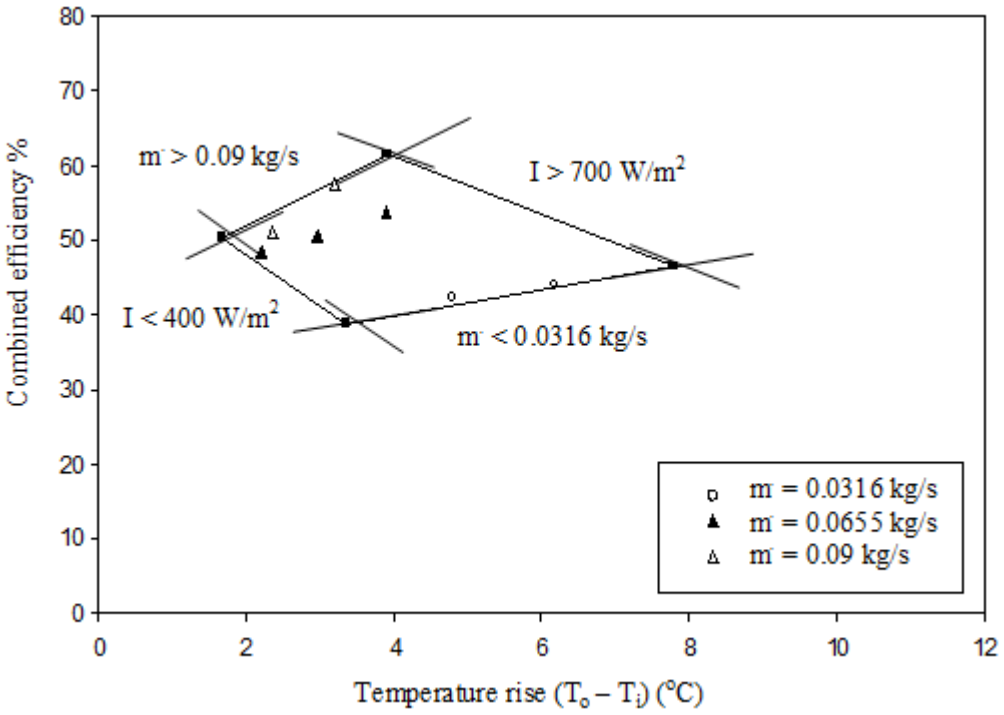

Figure 12: Effect of the temperature rise on the combined efficiency for single pass, double duct PV/T without CPC at various mass flow rates and [Ti = 30°C]

Conclusion :

This study presents the experimental and theoretical investigations of comprehensive configuration designs of dual passage photovoltaic thermal air collectors. Several conclusions are gathered. Increasing the mass flow rate will cause a increase in photovoltaic, thermal, and combined efficiencies of the PV/T collectors. Higher air mass flow rate will increase the heat transfer coefficient between channels wall and the air flow.

Increasing the value of heat transfer coefficient will cause the photovoltaic cell temperature and absorber plate to decrease. Decreasing the temperature will cause an increase in photovoltaic and thermal efficiencies of the PV/T collectors. Curves obtained from

different configuration designs show the effect of operating conditions on the efficiencies. Therefore, the curves would be useful to the designer to observe the effect of operating conditions on the efficiencies. Close agreement between experimental results and theory have been obtained. So, the mathematic model built is accepted and can be used to determine the performance of the PV/T collectors. The predicted outlet temperatures are within 2 to 5% compared to the experimental outlet temperature. It is expected that the collector with CPC and fins have higher efficiency than collector with fins only.

References:

1. Florschuetz, L.W. 1979. Extension of the Hottel-Whillier model to the analysis of combined photovoltaic thermal flate plate collectors. *Solar Energy* **22**: 227-241.
2. Cox, C.H., and Raghuraman, P. 1985. Design considerations for flat-plate photovoltaic/thermal collectors. *Solar Energy* **35**(3): 227-241.
3. Garg, H.P., Agarwal, R.K., and Bhargava, A.K. 1991. The effect of palne booster reflectors on the Performance of a Solar air heater with solar cells suitable for a solar dryer. *Energy Conversion* and *management* **35**(6): 543-554.
4. Prakash, J. 1994. Transient analysis of a photovoltaic-thermal solar collector for co-generation of electricity and hot air/water. *Energy Conversion & Management* **35**(11): 967-972.
5. Takashima, T., Tanaka, T., Doi, T. and Kamoshida, J. 1994. New proposal for photvoltaic-thermal solar energy utilization method. *Solar Energy* **52**(3): 241-245.

6. Garg, H.P., and Adhikari, R.S. 1997. Conventional hybrid photovoltaic/thermal (PV/T) air heating collectors: Steady state simulation. *Renewable Energy* **11**(30): 363-385.
7. Garg, H.P., and Adhikari, R.S. 1998. System performance studies on a photovoltaic/thermal (PV/T) air heating collector. *Renewable Energy* **16**(1-4): 725-730.
8. Tiwari, A., Sodha, M.S., Chandra, A., and Joshi, J.C. 2006. Performance evaluation of photovoltaic thermal solar air collector for composite climate of India. *Solar Energy Material & Solar Cells* **90**(2): 175–189.
9. Tonui, J.K., and Tripanagnostopoulos, Y. 2007a. Improved PV/T solar collectors with heat extraction by natural or forced air circulation. *Renewable Energy* **32**: 623–637.
10. Tonui, J.K. & Tripanagnostopoulos, Y. 2007b. Air-cooled PV/T solar collectors with low cost performance improvement. *Solar Energy* **81**: 498–511.
11. Tiwari, A., and Sodha, M.S. 2007. Parametric study of various configurations of hybrid PV/thermal air collector: experimental validation of theoretical model. *Solar Energy Materials and Solar Cells* **91**: 17–28.
12. Sopian, K., Yigit, K.S., Liu, H.T. Kakac, S. & Veziroglu, T.N. 1996. Performance analysis of photovoltaic thermal air heaters. *Energy Conversion and management* **37**(11): 1657-1670.
13. Garg, H.P., and Adhikari, R.S. 1999. Performance analysis of a hybrid photovoltaic/thermal (PV/T) collector with integrated CPC troughs. *International Journal of Energy Research* **23**:1295-1304.
14. Sopian, K., Liu, H.T., Kakac, S., and Veziroglu, T.N. 2000. Performance analysis of a double pass photovoltaic thermal

solar collector sutible for solar drying system. *Energy Conversion and management* **41**: 353-365.

15. Tripanagostopoulus, Y., Nousia, TH., Souliotis, M., and Yianoulis, P. 2002 hybrid photovoltaic/thermal Solar systems. *Solar Energy* **72**(3): 217-234.
16. Othman, M.Y., Yatim, B., Sopian, K., and Bakar, M.N. 2005. Performance studies on a finned double-pass photovoltaic-thermal (PV/T) solar collector. *Desalination* **209**: 43–49.
17. Sopian, K., Yigit, K.S., Liu, H.T. and Kakac, S. 1997 Research and development of hybrid photovoltaic thermal solar air heaters. *International Journal of Global energy* **9**: 382-392.